Journal of Biochemical and Biophysical Methods, 26 (1993) 1–26

JBBM 00972

NMR spectroscopic properties (^{1}H at 500 MHz) of deuterated* ribonucleotide-dimers ApU*, GpC*, partially deuterated 2′-deoxyribonucleotide-dimers d(TpA*), d(ApT*), d(GpC*) and their comparison with natural counterparts (^{1}H-NMR window)

A. Földesi, F.P.R. Nilson, C. Glemarec, C. Gioeli and J. Chattopadhyaya

Department of Bioorganic Chemistry, Biomedical Center, University of Uppsala, Uppsala (Sweden)

(Received 28 July 1992)
(Revised version received 17 August 1992)
(Accepted 1 September 1992)

Summary

Pure 1′$^{\#}$,2′,3′,4′$^{\#}$,5′,5′′-$^2H_6$-ribonucleoside derivatives **10–14**, 1′$^{\#}$,2′,2″,3′,4′$^{\#}$,5′,5″-$^2H_7$-2′-deoxynucleoside blocks **15–18** and their natural-abundance counterparts were used to assemble partially deuterated ribonucleotide-dimers (* indicates deuteration at 1′$^{\#}$,2′,3′,4′$^{\#}$,5′,5″($^2H_6$)): ApU* **21**, GpC* **22** and partially deuterated 2′-deoxyribonucleotide-dimers d(TpA*) **23**, d(ApT*) **25**, d(GpC*) **26** (* indicates deuteration at 1′$^{\#}$, 2′,2″,3′,4′$^{\#}$,5′,5″($^2H_7$)) according to the procedure described by Földesi et al. (Tetrahedron, in press). These five partially deuterated oligonucleotides were subsequently compared with their corresponding natural-abundance counterparts by 500 MHz ^{1}H-NMR spectroscopy to evaluate the actual NMR simplifications achieved in the non-deuterated part (^{1}H-NMR window) as a result of specific deuterium incorporation. Detailed one-dimensional ^{1}H-NMR (500 MHz), two-dimensional correlation spectra (DQF-COSY and TOCSY) and deuterium isotope effect on the chemical shifts of oligonucleotides have been presented.

Key words: ^{1}H-NMR spectroscopy; Deuterated ribonucleotide dimer; Deuterated 2′-deoxyribonucleotide dimer

RNA and DNA have a large number of biological function such as storage and propagation of genetic information or catalytic activity. These DNA and RNA molecules have different secondary (double strands, hairpin loops, internal loops,

Correspondence address: J. Chattopadhyaya, Department of Bioorganic Chemistry, Box 581, Biomedical Center, University of Uppsala, S-751 23 Uppsala, Sweden.

bulges) and tertiary (triple strands, helical junctions, pseudoknots) structural elements [1] that are connected to the specific biological functions. The study of the conformational behaviour of these macromolecules would most probably help us to understand how the conformational characteristics of DNA and RNA translate into interaction and recognition that culminate into specific biological function. Nuclear magnetic resonance (NMR) spectroscopy has emerged as one of the most powerful tools [2] in conjunction with various computational methods [2–6] which provide conformational information under biological condition. In this complex approach to solve the problem of solution geometry of DNA or RNA molecules, the NMR measurements provide the informations on bond torsion angles and interproton distances as inputs for the computational calculations for model building. The information on bond torsion can be extracted from homonuclear two-dimensional (2-D) correlated spectroscopy (COSY) providing a direct proof of the existence of resolved scalar couplings ($^3J_{HH}$), and correlates the chemical shifts of coupling partner through the single or multiple coherence transfer of nuclear spins as in DQF-COSY or by HOHAHA or TOCSY which visualize the structure of the spin system in a most direct and informative manner [2c,4]. The information on interproton distances are derived from 2-D nuclear Overhauser enhancement (NOESY) [5] results which indicate through-space interactions between two relaxing protons [5b–e]. In an effort to collect these primary conformational informations, it would be ideal that each resonance line and cross-peak due to two interacting nuclei is clearly separated in homonuclear proton-proton, heteronuclear proton-carbon, proton-phosphorus, carbon-phosphorus, NOESY and ROESY experiments. Enormous developments both in hardware (increasing magnetic field, more powerful computers) and spectral editing methods [2f,4,6] allow us to partly tackle the problem of spectral complexity due to resonance overlap and allow the extraction of $^3J_{HH}$ and nOe volumes in an unambiguous manner from up to 14–16-mer duplex DNA and 8–12-mer single stranded RNA but it is simply impossible to collect all of these informations in a non-prejudicial manner from a larger molecule. Clearly, these problems are associated with spectral overlap which becomes more and more complex due to overcrowding of resonances particularly from the repeating pentose moieties with increasing chain length. The problem due to severe spectral overlap of proton resonances in absorption assignments and in measurements of $^3J_{HH}$ and nOe volume of a larger biologically functional DNA or RNA molecule could be solved by chemical means by substituting proton (^1H) with deuteron (^2H) in a chosen domain and extracting necessary information arising from the shorter NMR-visible non-deuterated part (^1H-NMR window). By incremental shift of the ^1H-NMR window in a series of oligo-DNA or RNA with identical sequence (Scheme 1), one should be able to put together the total structural information of a much larger oligonucleotide than what is possible today. The most important part in this concept is that two ^1H-NMR windows in two oligomers of the series should have at least an overlap of a nucleotide residue with specific chemical shifts in order to be able to correlate protons from both windows with respect to the same nucleotide reference point (i.e. same proton resonances in both NMR-windows).

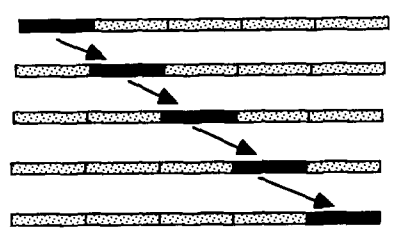

Succesive shift of "NMR-window" in a DNA or RNA molecule allows the incremental assemblage of conformational information such as torsional angles or nOes using the techniques of Multidimensional NMR spectroscopy

"NMR-window" = Non-deuterated DNA/RNA

Deuterated DNA/RNA

Signifies shift of "NMR-window" across the whole length of the molecule.
Note that the design of NMR-windows with a slight overlap enables one to walk on the molecule by a common nOe or a chemical shift on two adjacent "NMR-windows"

Scheme 1

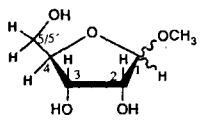

1

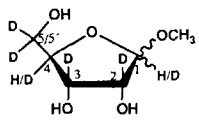

2

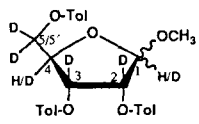

3

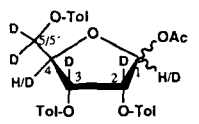

4

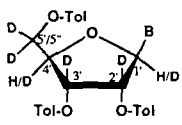

5: B = U
6: B = C^{Bz}
7: B = A^{Bz}
8: B = G^{DPC}_{Ac}
9: B = T

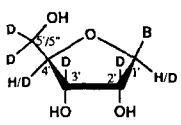

10: B = U
11: B = C^{Bz}
12: B = A^{Bz}
13: B = G^{DPC}_{Ac}
14: B = T

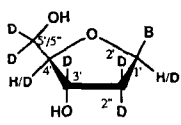

15: B = C^{Bz}
16: B = A^{Bz}
17: B = G^{DPC}_{Ac}
18: B = T

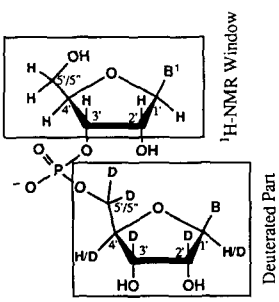

19: B^1 = U; B = A
20: B^1 = C; B = G
21: B^1 = A; B = U
22: B^1 = G; B = C

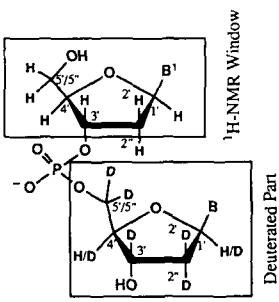

23: B^1 = T; B = A
24: B^1 = C; B = G
25: B^1 = A; B = T
26: B^1 = G; B = C

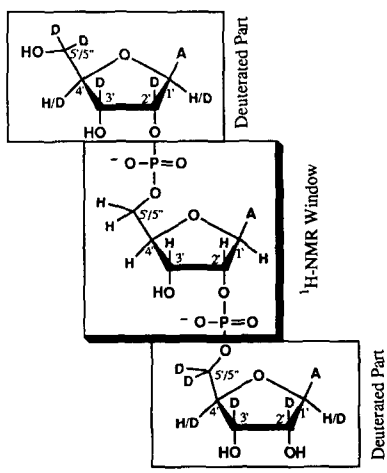

27

where: Tol = 4-toluoyl, Ac = acetyl, U = uracil-1-yl, C^{Bz} = N^4-benzoylcytosin-1-yl, A^{Bz} = N^6-benzoyladenin-9-yl, G^{DPC}_{Ac} = N^2-acetyl-O^6-diphenylcarbamoylguanin-9-yl, T = thymin-1-yl, A = adenin-9-yl, C = cytosin-1-yl, G = guanin-9-yl

Scheme 2

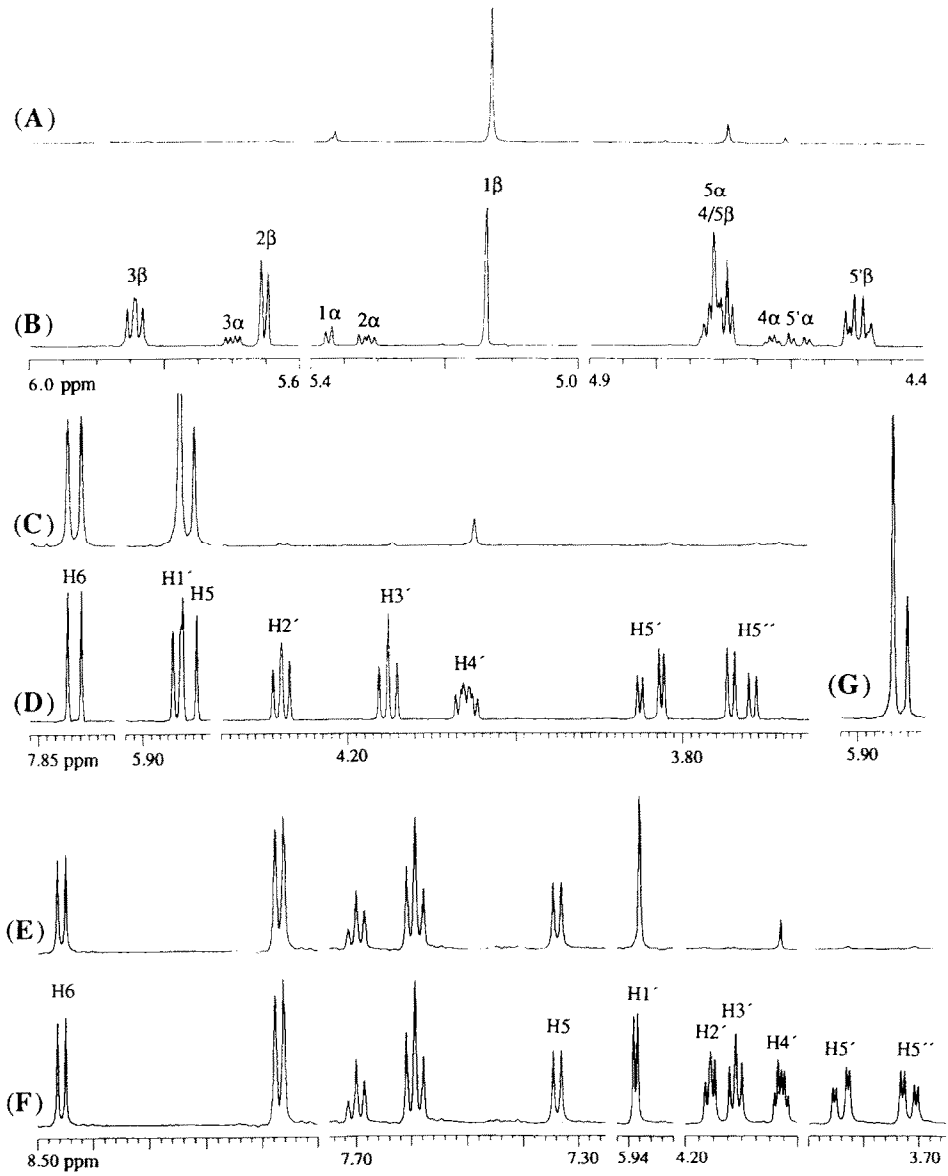

Fig. 1. 500 MHz ^{1}H-NMR spectra of deuterated D-ribofuranose (> 97 atom % ^{2}H at C2, C3, C5/5'; ~ 85 atom % ^{2}H at C4; ~ 20 atom % ^{2}H at C1), deuterated-β-D-nucleosides and their natural-abundance counterparts (99.985 atom % ^{1}H). (A) shows 1-*O*-methyl-2,3,5-tri-*O*-(4-toluoyl)-(α/β: ~ 1/10)-D-ribofuranoside (**3**) and (B) shows its natural-abundance counterpart. (C) shows 1'$^{\#}$,2',3',4'$^{\#}$,5',5''-$^2H_6$-uridine (**10**); (D) shows natural-abundance counterpart; (G) shows the full height anomeric region of 1'$^{\#}$,2',3',4'$^{\#}$,5',5''-$^2H_6$-uridine (**10**) from subspectrum (C). (E) shows 1'$^{\#}$,2',3',4'$^{\#}$,5',5''-$^2H_6$-N^4-benzoylcytidine (**11**); (F) shows natural-abundance counterpart.

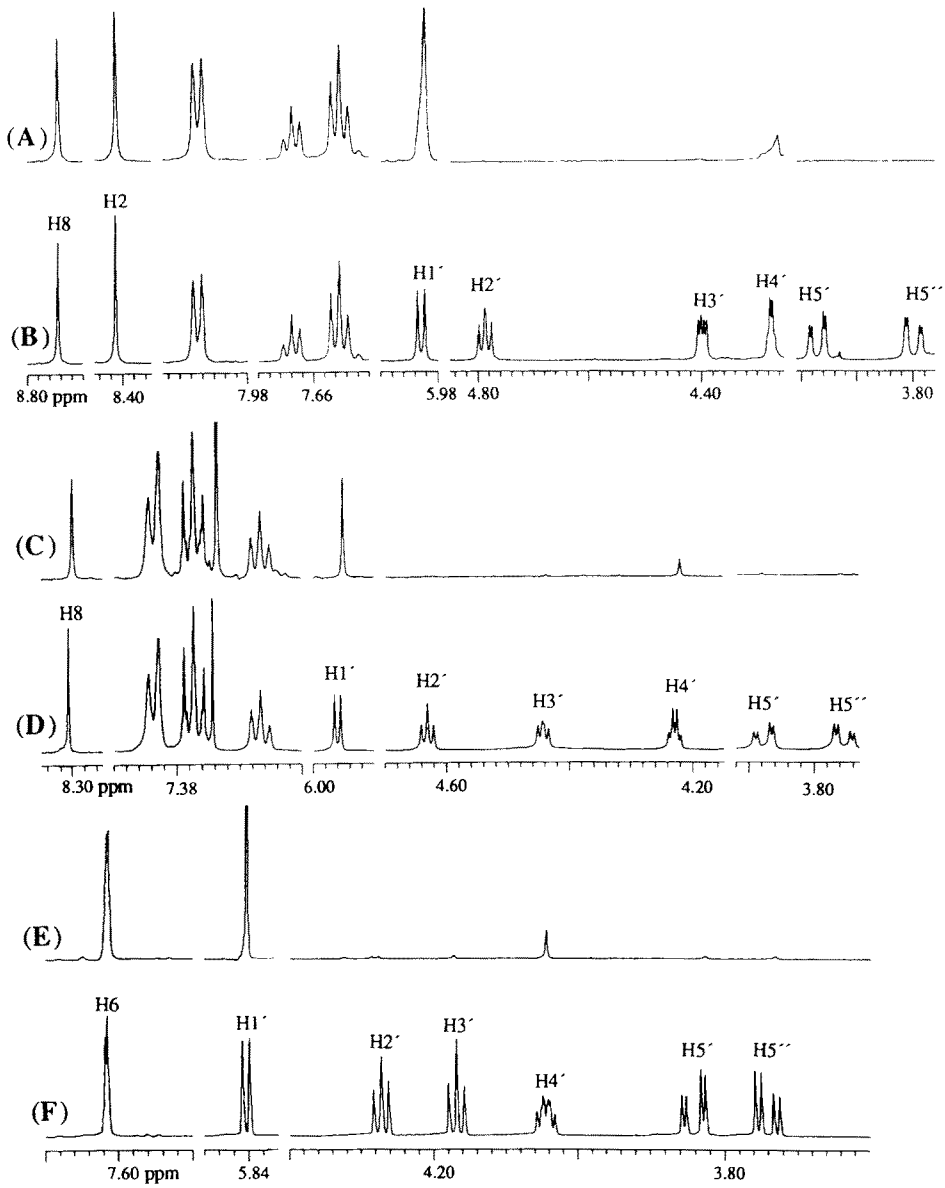

Fig. 2. 500 MHz ^{1}H-NMR spectra of deuterated-β-D-nucleosides (> 97 atom % ^{2}H at C2′, C3′, C5′/5″; ~ 85 atom % ^{2}H at C4′ (C4′$^{\#}$); ~ 20 atom % ^{2}H at C1′ (C1′$^{\#}$)) and their natural-abundance counterparts (99.985 atom % ^{1}H). (A) shows 1′$^{\#}$,2′,3′,4′$^{\#}$,5′,5″-$^2H_6$-N^6-benzoyladenosine (**12**); (B) shows natural-abundance counterpart. (C) shows 1′$^{\#}$,2′,3′,4′$^{\#}$,5′,5″-$^2H_6$-N^2-acetyl-O^6-diphenylcarbamoylguanosine (**13**); (D) shows natural-abundance counterpart. (E) shows 1-(1′$^{\#}$,2′,3′,4′$^{\#}$,5′,5″-$^2H_6$-β-D-ribofuranosyl)-thymine (**14**): (F) shows natural-abundance counterpart.

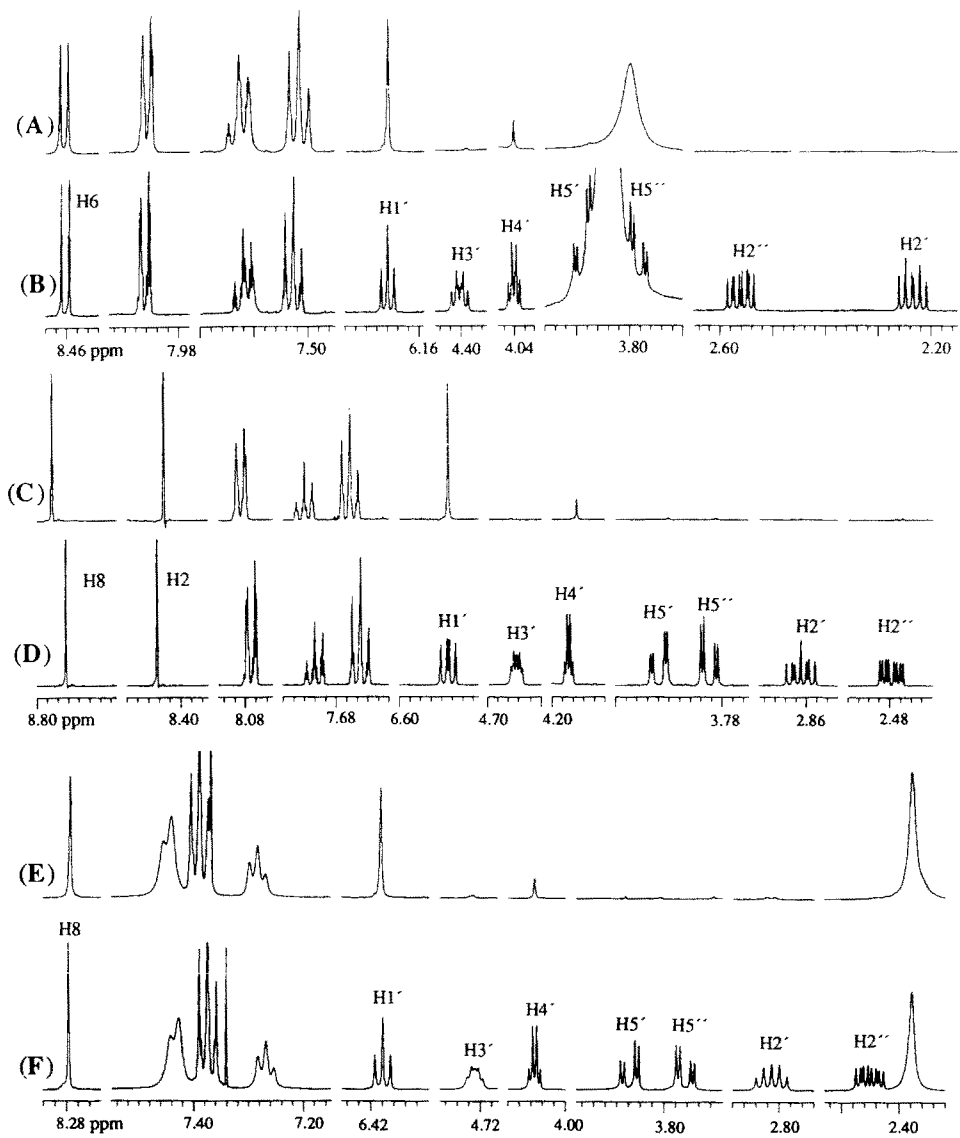

Fig. 3. 500 MHz ^{1}H-NMR spectra of deuterated-β-D-nucleosides (> 97 atom % ^{2}H at C2′, C3′, C5′/5″; ~ 85 atom % ^{2}H at C4′ (C4′$^{\#}$); ~ 20 atom % ^{2}H at C1′ (C1′$^{\#}$)) and their natural-abundance counterparts (99.985 atom % ^{1}H). (A) shows 1′$^{\#}$,2′,2″,3′,4′$^{\#}$,5′,5″-$^2H_7$-2′-deoxy-N^4-benzoylcytidine (**15**); (B) shows natural-abundance counterpart. (C) shows 1′$^{\#}$,2′,2″,3′,4′$^{\#}$,5′,5″-$^2H_7$-2′-deoxy-N^6-benzoyladenosine (**16**); (D) shows natural-abundance counterpart. (E) shows 1′$^{\#}$,2′,2″,3′,4′$^{\#}$,5′,5″-$^2H_7$-2′-deoxy-N^2-acetyl-O^6-diphenylcarbamoylguanosine (**17**); (F) shows natural-abundance counterpart.

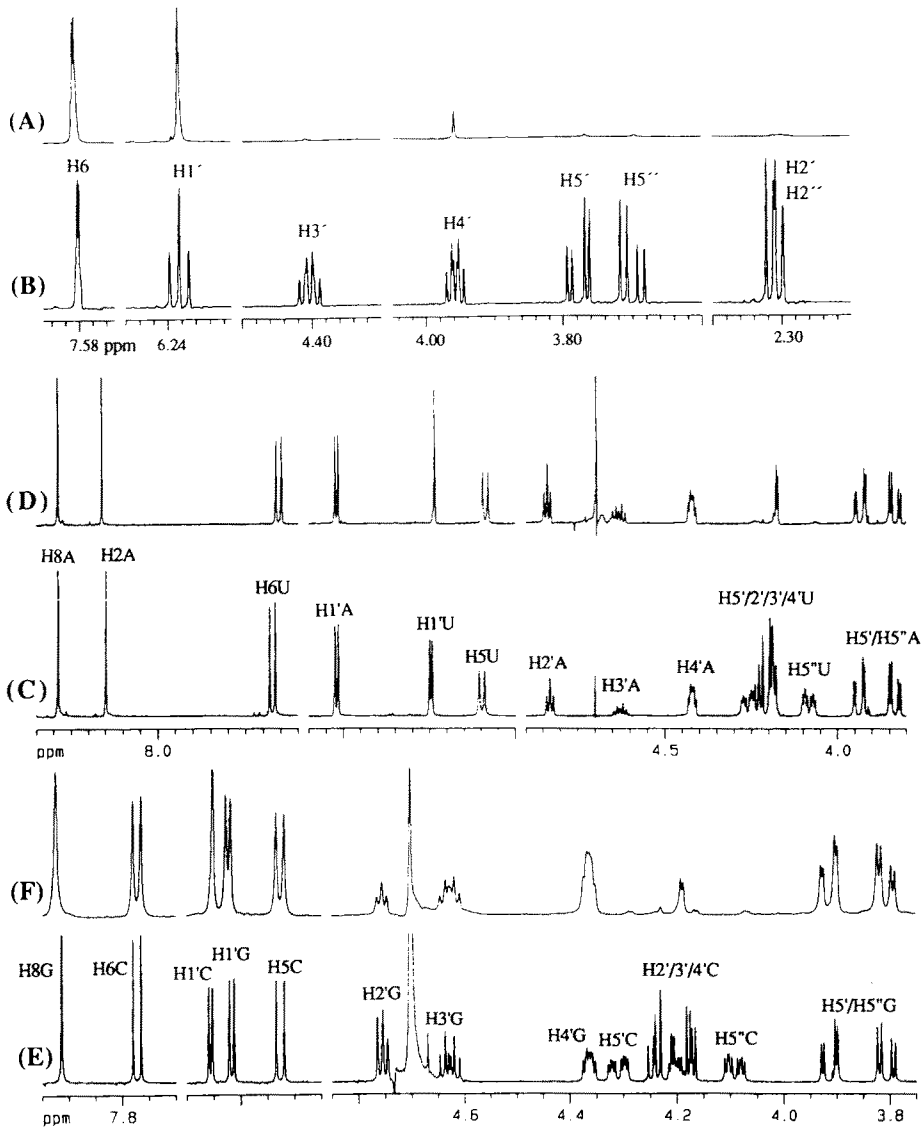

Fig. 4. 500 MHz ^{1}H-NMR spectra of deuterated-β-D-nucleoside (> 97 atom % ^{2}H at C2′, C3′, C5′/5″; ~ 85 atom % ^{2}H at C4′ (C4′$^{\#}$); ~ 20 atom % ^{2}H at C1′ (C1′$^{\#}$)) and its natural-abundance counterpart (99.985 atom % ^{1}H) and natural and partially deuterated diribonucleoside-(3′ → 5′)-monophosphates in D_2O at 298 K. (A) shows 1′$^{\#}$,2′,2″,3′,4′$^{\#}$,5′,5″-$^2H_7$-thymidine (**18**); (B) shows natural-abundance counterpart. (C): natural ApU, (D): ApU* where the 1′$^{\#}$,2′,3′,4′$^{\#}$ and 5′/5″ protons of the uridine (pU*) residue are exchanged with ^{2}H. (E): natural GpC, (F): GpC* where the 1′$^{\#}$,2′,3′,4′$^{\#}$ and 5′/5″ protons of the cytidine (pC*) residue are exchanged with ^{2}H. The H1′$^{\#}$ appears as a singlet while the H4′$^{\#}$ appears as a doublet due to its coupling to the phosphorus of the 3′ → 5′ phosphate linkage.

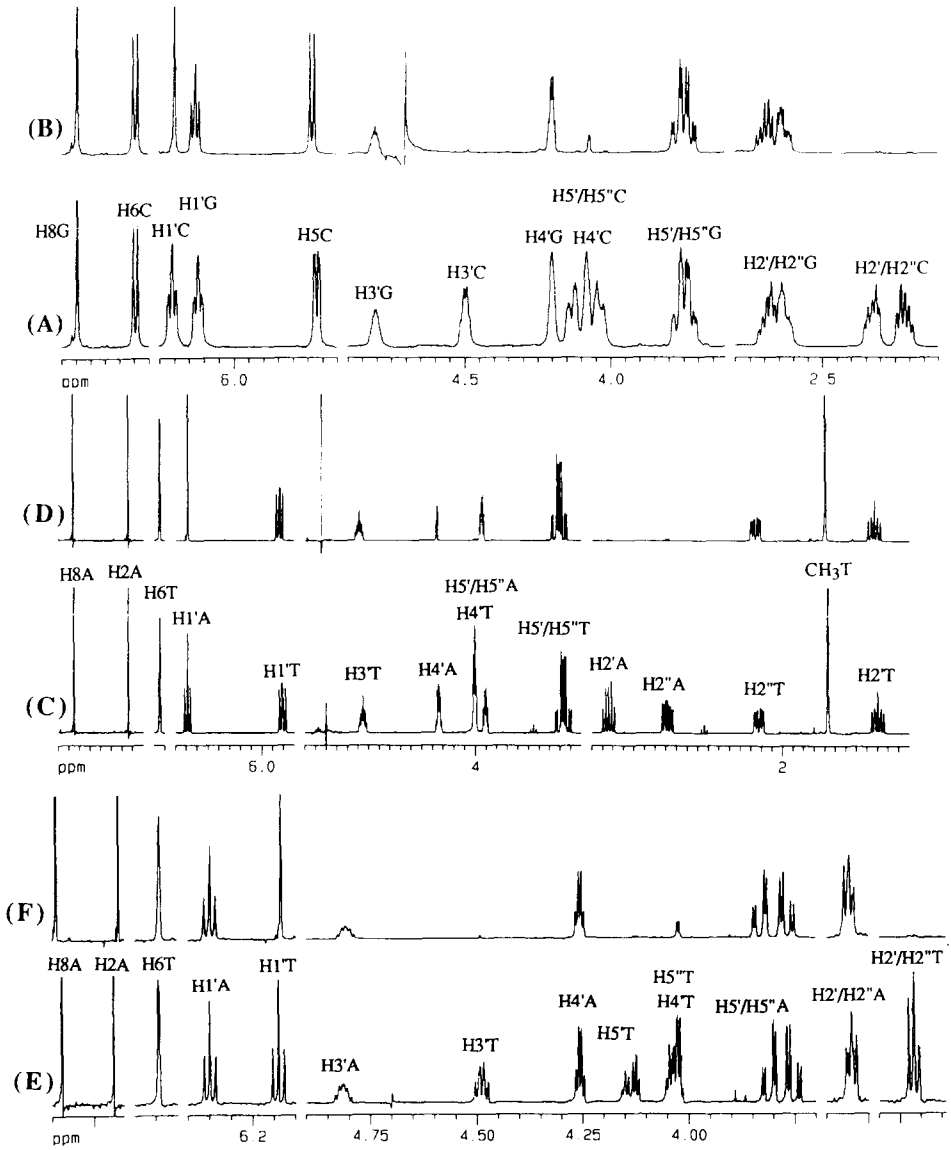

Fig. 5. ^{1}H-NMR spectra of natural and partially deuterated di(2′-deoxyribonucleoside)-(3′ → 5′)-monophosphates in D_2O at 298 K. (A): natural d(GpC), (B): d(GpC*) where the 1′$^{\#}$,2′,2″,3′,4′$^{\#}$ and 5′/5″ protons of the cytidine (pC*) residue are exchanged with ^{2}H. (C): natural d(ApT), (D): d(ApT*) where the 1′$^{\#}$,2′,2″,3′,4′$^{\#}$ and 5′/5″ protons of the thymidine (pT*) residue are exchanged with ^{2}H. (E): natural d(TpA), (F): d(TpA*) where the 1′$^{\#}$,2′,2″,3′,4′$^{\#}$ and 5′/5″ protons of the adenosine (pA*) residue are exchanged with ^{2}H. The H1′$^{\#}$ appears as a singlet while the H4′$^{\#}$ appears as a doublet due to its coupling to the phosphorus of the 3′ → 5′ phosphate linkages.

Although nucleosides have been selectively deuterated with very different amount of deuterium incorporation at both sugar [7] and nucleoside [8] levels using different chemical [7b–g,i–n,8a–g,10a,12] and enzymatic [7h,8h–m] methods, these monomers have not really found their application in conformational studies on

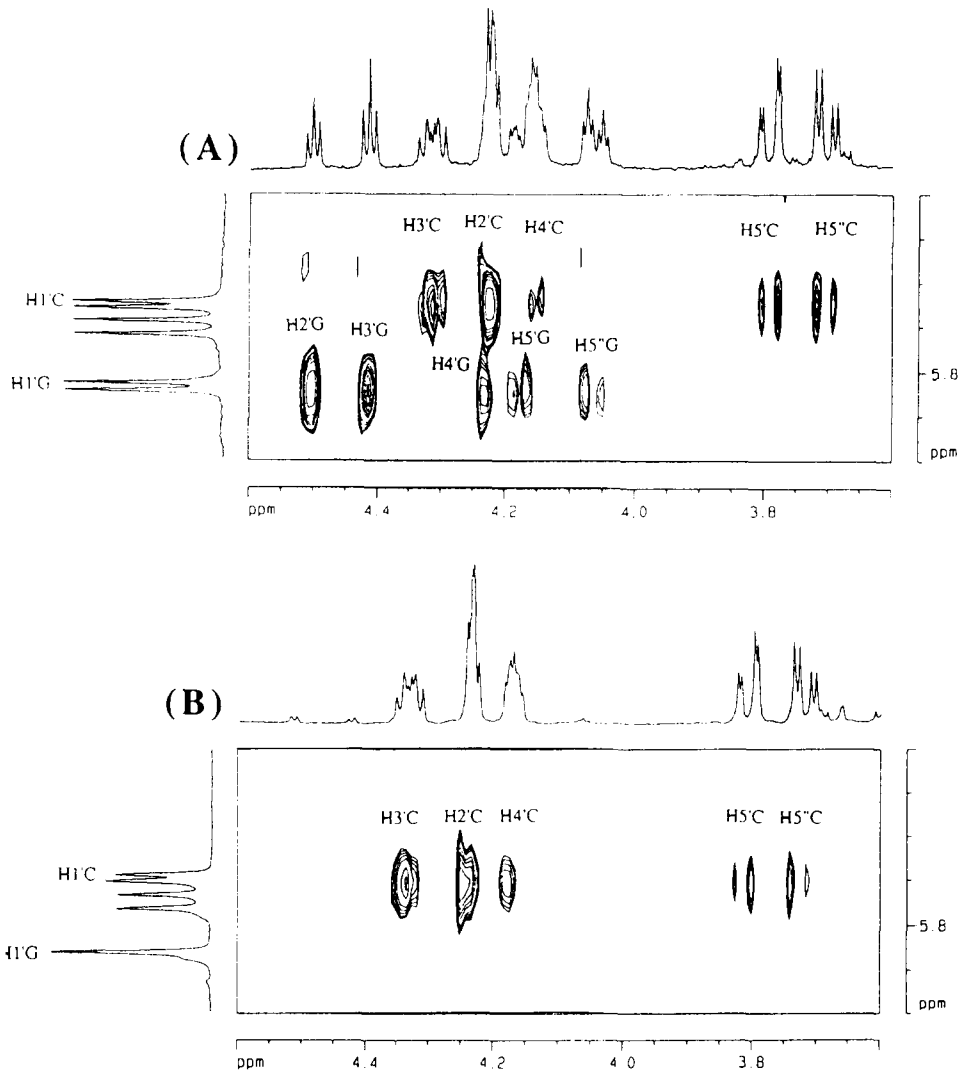

Fig. 6. HOHAHA spectra of the natural and partially deuterated cytidylyl-(3′ → 5′)-guanosine (CpG) in D_2O at 298 K. Panel A represents the 2-D spectrum for the non-deuterated CpG. Panel B represents the 2-D spectrum of the partially deuterated CpG* where the 1′#,2′,3′,4′# and 5′/5″ protons of the guanosine residue (pG*) are exchanged. In the 1-D spectrum, the H1′ appears as a singlet at 5.81 ppm while the H4′ appears as a doublet at 4.2 ppm due to its coupling to the phosphorus of the 3′ → 5′ phosphate linkage. In the 2-D spectrum, the J-network for the 3′-terminal residue has vanished.

oligonucleotides. Examples of base deuteration [9] and its effect on the 2-D ^{1}H-NMR and ^{2}H-NMR studies on oligomers selectively deuterium labeled at given positions of the sugar moiety [10] are known. The most detailed studies on various dimers and trimers where one of the nucleotide units was fully enzymatically

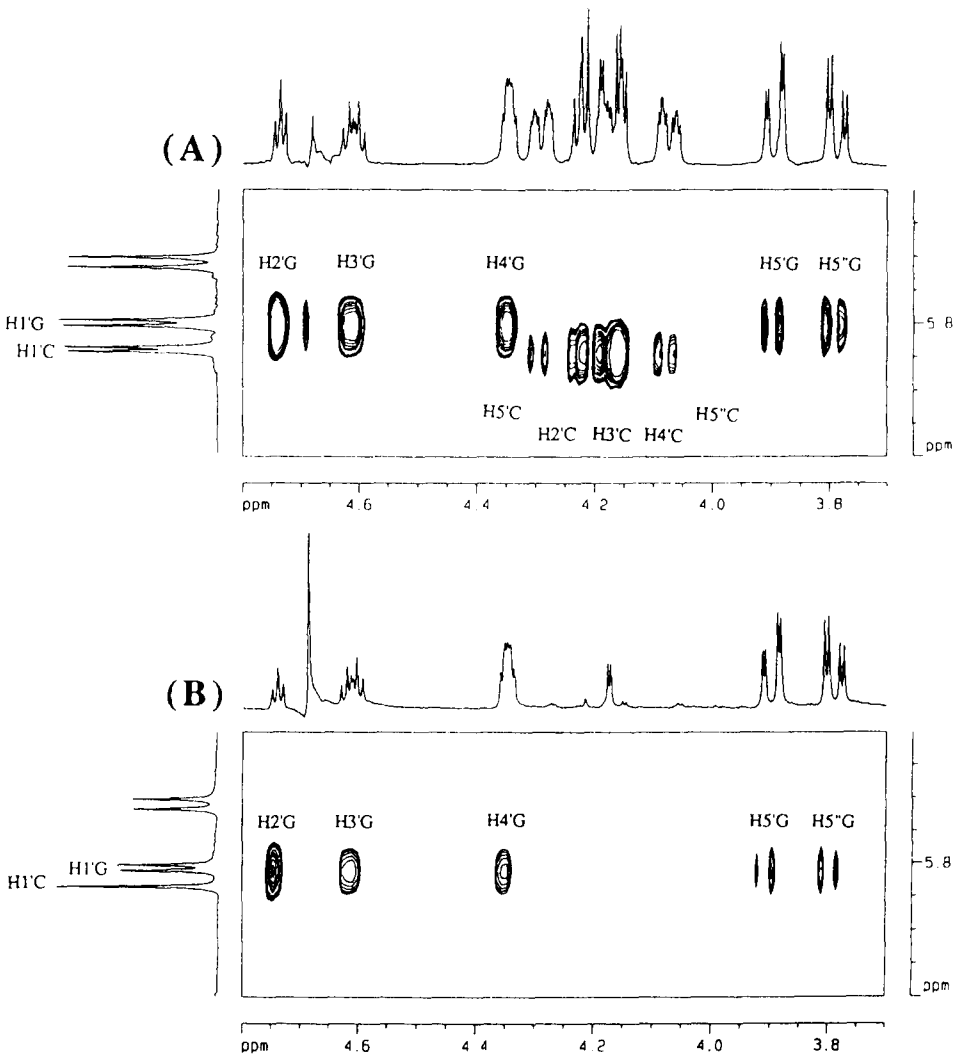

Fig. 7. HOHAHA spectra of the natural and partially deuterated guanylyl-(3′ → 5′)-cytidine (GpC) in D_2O at 298 K. Panel A represents the 2-D spectrum for the non-deuterated GpC. Panel B represents the 2-D spectrum of the partially deuterated GpC* where the 1′$^{\#}$,2′,3′,4′$^{\#}$ and 5′/5″ protons of the cytidine (pC*) residue are exchanged. In the 1-D spectrum, the H1′ appears as a singlet at 5.84 ppm while the H4′ appears as a doublet at 4.2 ppm due to its coupling to the phosphorus of the 3′ → 5′ phosphate linkage. In the 2-D spectrum, the J-network for the 3′-terminal residue has vanished.

deuterated were carried out in the early seventies when the 2-D spectroscopy was not developed yet [8h–m]. This lack of data on the required level of deuteration necessary in the pentose sugar moieties in nucleotides for effective suppression of cross-peaks in 2-D NMR spectroscopy, in general, and how such deuteration may

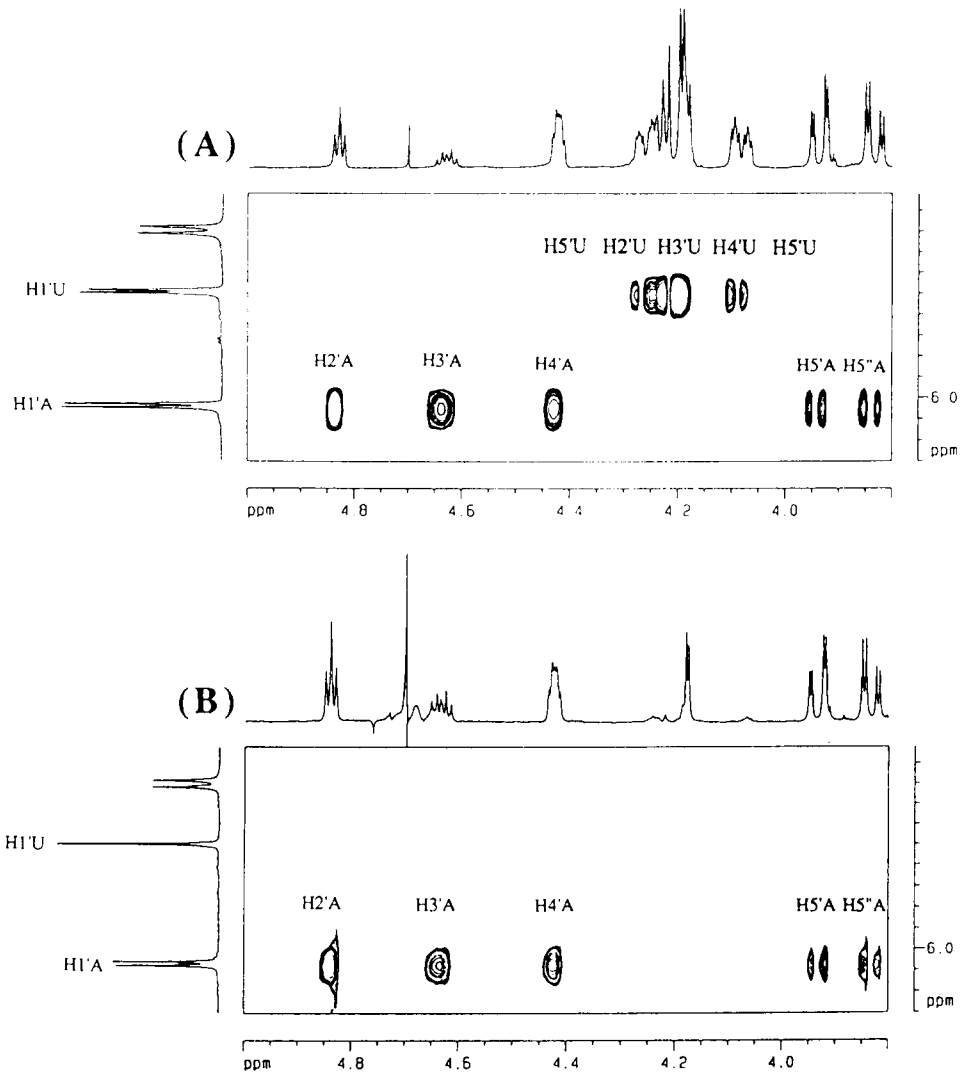

Fig. 8. HOHAHA spectra of the natural and partially deuterated adenylyl-(3′ → 5′)-uridine (ApU) in D_2O at 298 K. Panel A represents the 2-D spectrum for the non-deuterated ApU. Panel B represents the 2-D spectrum of the partially deuterated ApU* where the 1′#,2′,3′,4′# and 5′/5″ protons of the uridine (pU*) residue are exchanged. In the 1-D spectrum, the H1′ appears as a singlet at 5.75 ppm while the H4′ appears as a doublet at 4.15 ppm due to its coupling to the phosphorus of the 3′ → 5′ phosphate linkage. In the 2-D spectrum, the J-network for the 3′-terminal residue (pU*) has vanished.

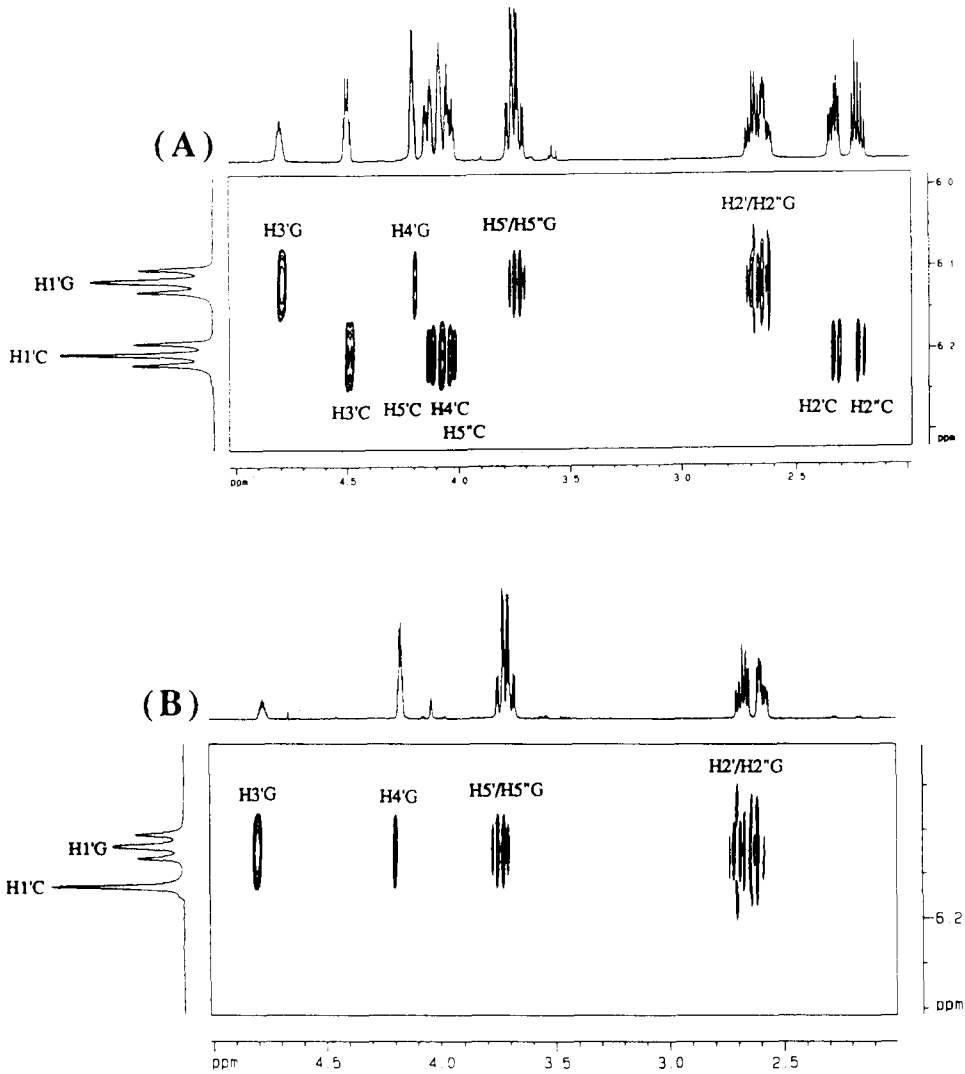

Fig. 9. HOHAHA spectra of the natural and partially deuterated 2′-deoxyguanylyl-(3′ → 5′)-2′-deoxycytidine [d(GpC)] in D_2O at 298 K. Panel A represents the 2-D spectrum for the non-deuterated d(GpC). Panel B represents the 2-D spectrum of the partially deuterated d(GpC*) where the 1′#,2′,2″,3′,4′# and 5′/5″ protons of the cytidine (pC*) residue are exchanged. In the 1-D spectrum, the H1′ appears as a singlet at 6.19 ppm while the H4′ appears as a doublet at 4.1 ppm due to its coupling to the phosphorus of the 3′ → 5′ phosphate linkage. In the 2-D spectrum, the J-network for the 3′-terminal residue has vanished.

cause spectral simplification has promted us to take up this study on ^{1}H-NMR window (Scheme 1) [11].

Our synthetic strategy [11] involved deuteration of methyl α/β-D-ribofuranoside **1** by Raney nickel-^2H_2O exchange reaction [7k–m,12] to give methyl 1#,2,3,4#,5,5′-$^2H_6$-α/β-D-ribofuranoside **2** (> 97 atom % ^{2}H at C2, C3, C5/5′; ~ 85 atom %

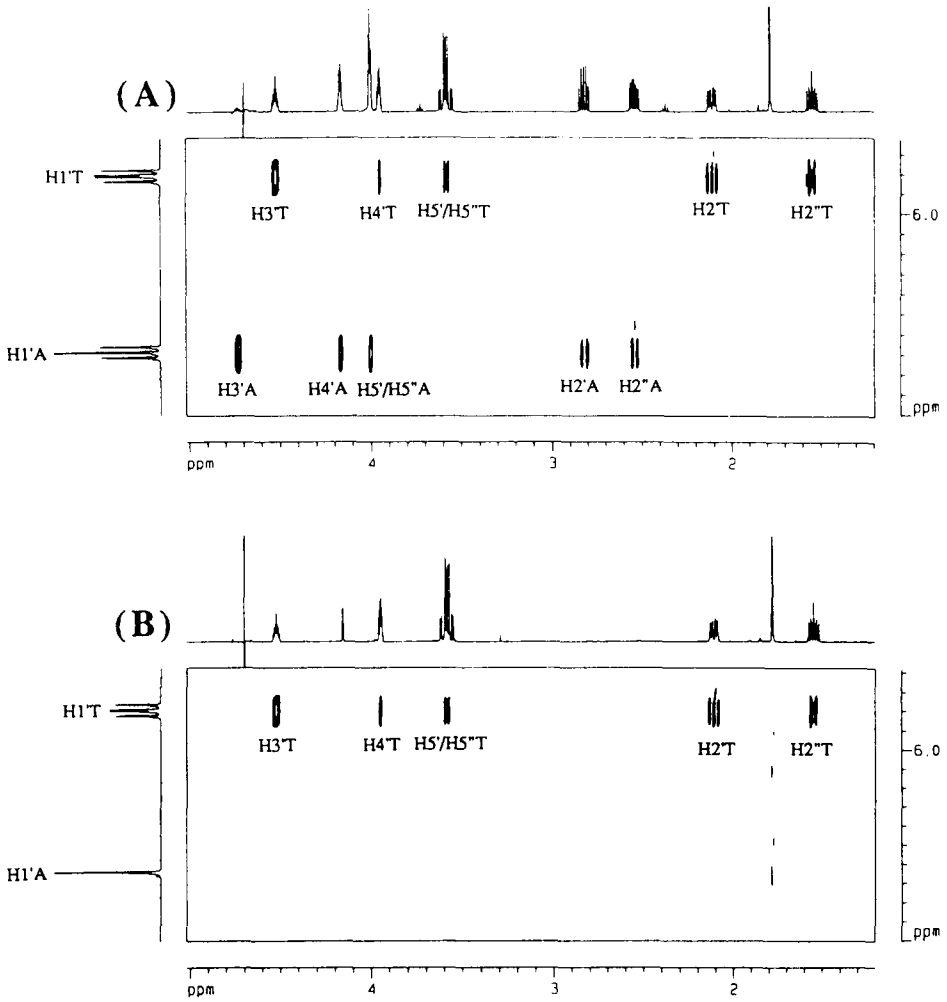

Fig. 10. HOHAHA spectra of the natural and partially deuterated thymidylyl-(3′ → 5′)-2′-deoxyadenosine [d(TpA)] in D_2O at 298 K. Panel A represents the 2-D spectrum for the non-deuterated d(Tpa). Panel B represents the 2-D spectrum of the partially deuterated d(TpA*) where the 1′#,2′,2″,3′,4′# and 5′/5″ protons of the adenosine (pA*) residue are exchanged. In the 1-D spectrum, the H1′ appears as a singlet at 6.38 ppm while the H4′ appears as a doublet at 4.10 ppm due to its coupling to the 3′ → 5′ phosporus of the phosphate linkage. In the 2-D spectrum, the J-network for the 3′-terminal residue has vanished.

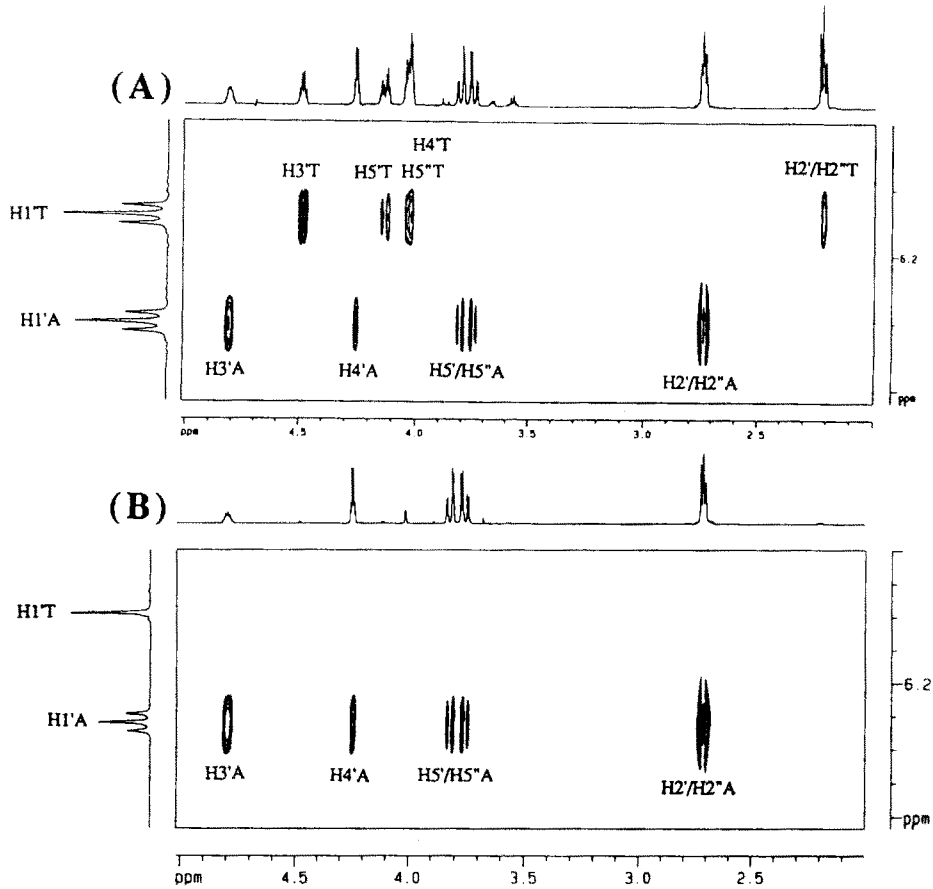

Fig. 11. HOHAHA spectra of the natural and partially deuterated 2′-deoxyadenylyl-(3′ → 5′)-thymidine (d(ApT)) in D_2O at 298 K. Panel A represents the 2-D spectrum for the non-deuterated d(ApT). Panel B represents the 2-D spectrum of the partially deuterated d(ApT*) where the $1'^{\#}$,2′,3′,$4'^{\#}$ and 5′/5″ protons of the thymidine (pT*) residue are exchanged. In the 1-D spectrum, the H1′ appears as a singlet at 6.15 ppm while the H4′ appears as a doublet at 4.00 ppm due to its coupling to the phosphorus of the 3′ → 5′ phosphate linkage. In the 2-D spectrum, the J-network for the 3′-terminal residue has vanished.

Fig. 12. DQF-COSY spectra of the natural and partially deuterated adenylyl-(3′ → 5′)-uridine (ApU) in D_2O at 298 K. Panel A: 2-D spectrum of the natural ApU. The cross peaks used for the determination of the vicinal $^3J_{HH}$ coupling constants are shown in the numbered boxes: (1) H1′-H2′A, (2) H2′-H3′A, (3) H3′-H4′A, (4) H4′-H5′A, H4′-H5″A, (5) H1′-H2′U, (6) H2′-H3′, H3′-H4′, H4′-H5′ and H4′-H5″U. Panel B: 2-D spectrum of ApU* where the $1'^{\#}$,2′,3′,$4'^{\#}$ and 5′/5″ of pU* have been exchanged with deuterium. The empty boxes show that all cross peaks involving the pU* residue have vanished.

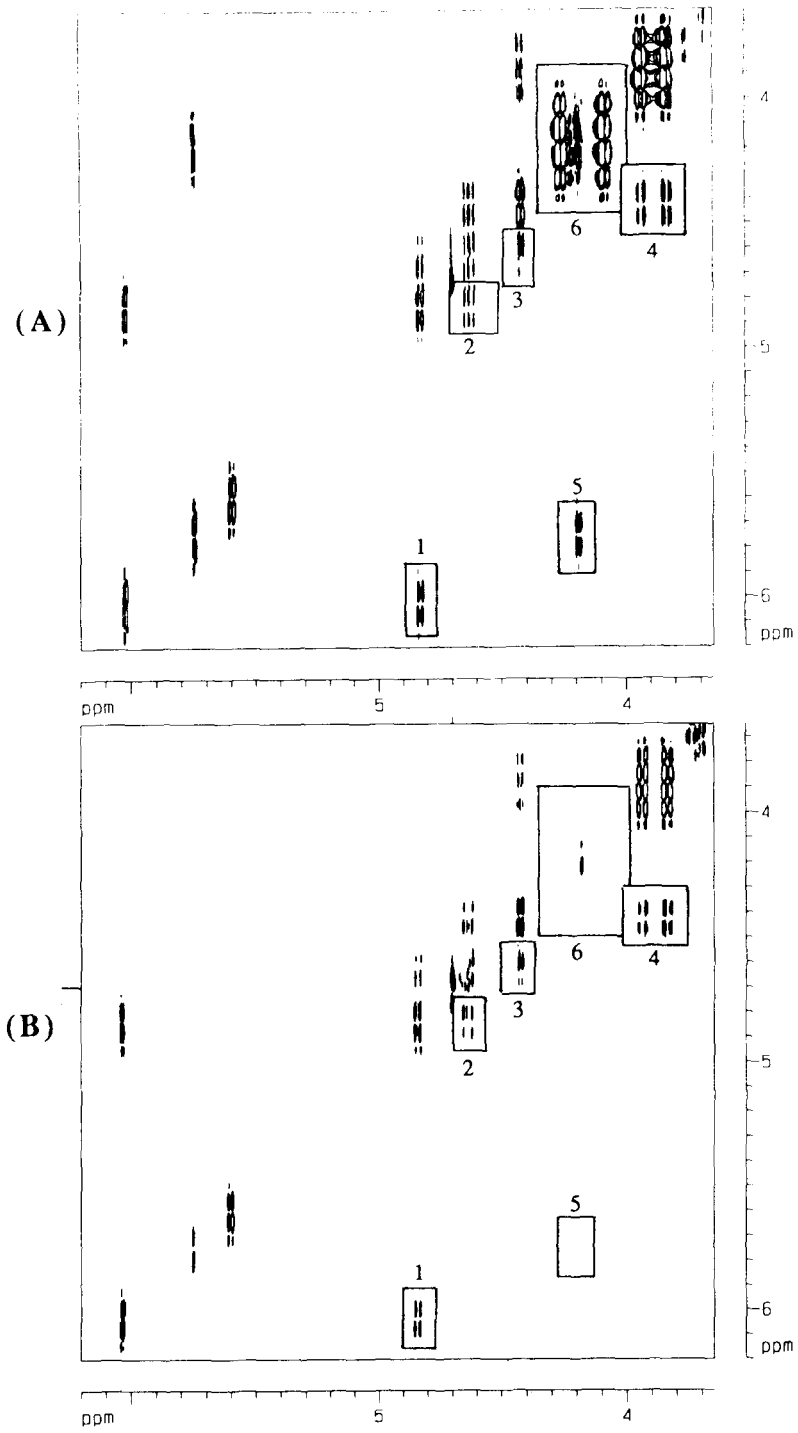
(A)
1
2
3
4
5
6
4
5
6
ppm
ppm
5
4
(B)
1
2
3
4
5
6
4
5
6
ppm
ppm
5
4

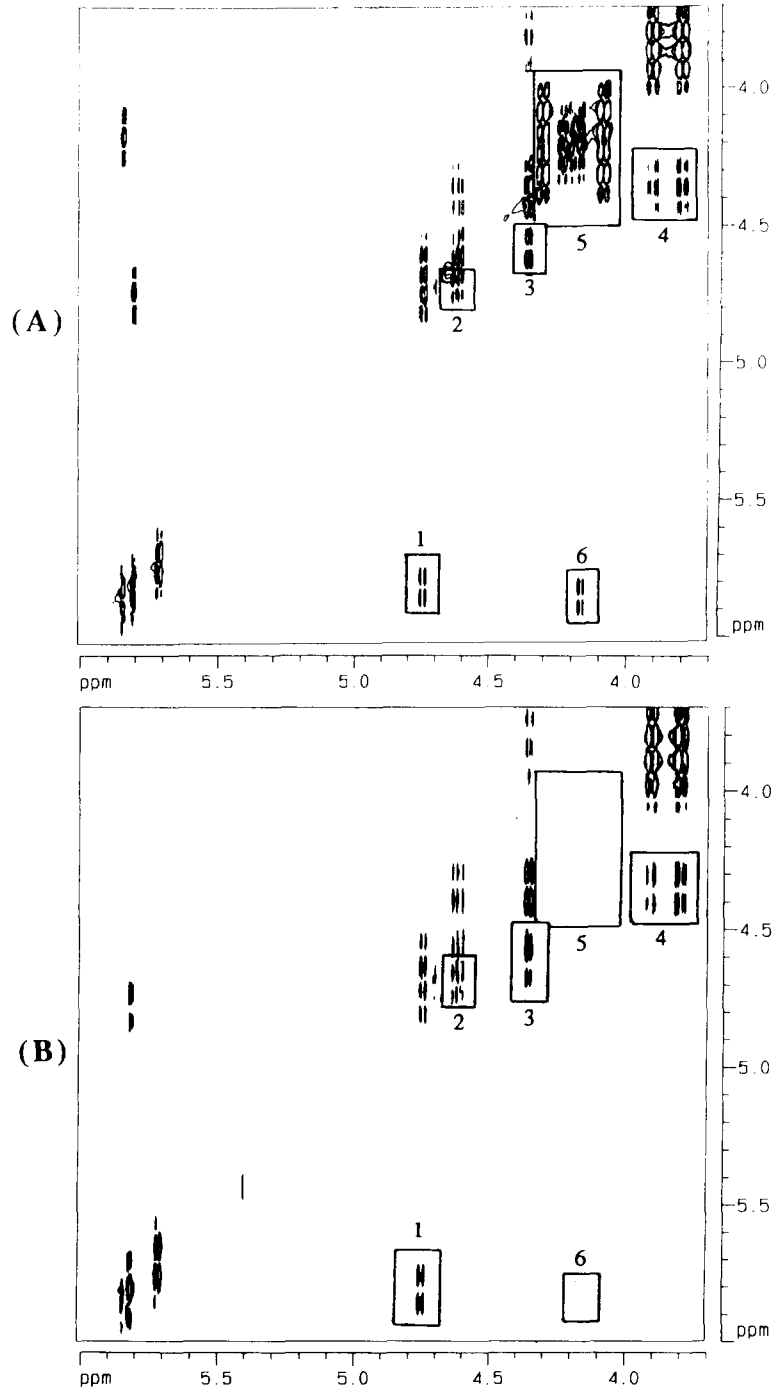

Fig. 13. DQF-COSY spectra of the natural and partially deuterated guanylyl-(3′ → 5′)-cytidine (GpC) in D_2O at 298 K. Panel A: 2-D spectrum of the natural GpC. The cross peaks used for the determination of the vicinal $^3J_{HH}$ coupling constants are shown in the numbered boxes: (1) H1′C-H2′G, (2) H3′C-H4′G, (3) H, (4) H4′-H5′, H4′-H5″G, (5) H1′-H2′C, H2′-H3′C, H3′-H4′C, H4′-H5′C and H4′-H5″C. Panel B: 2-D spectrum of GpC* where the $1'^{\#}$,2′,3′,$4'^{\#}$ and 5′/5″ of pC* have been exchanged with deuterium. The empty boxes show that all cross peaks involving the pC* residue have vanished.

^{2}H at C4 (C4′$^{\#}$); ~ 20 atom % ^{2}H at C1 (C1′$^{\#}$), $^{\#}$ denotes partial deuteration) as main product, which was purified after toluoylation of the hydroxyl groups (see Scheme 2). The 500 MHz ^{1}H-NMR spectrum of this deuterated sugar derivative **3** is shown in Fig. 1A to illustrate [11] the purity and deuteration level achieved. Subsequent 1-acetylation of this product resulted in 1-*O*-acetyl-2,3,5-tri-*O*-toluoyl-α/β-D-1$^{\#}$,2,3,4$^{\#}$,5,5′-$^2H_6$-ribofuranoside **4**, which was condensed with silylated nucleobases uracil, N^4-benzoylcytosine, N^6-benzoyladenine, N^2-acetyl-O^6-diphenylcarbamoyl guanine and thymine [11] to afford the ribonucleoside blocks **5–9**. The toluoyl groups from the fully protected nucleoside blocks were removed in a regioselective manner to give nucleobase protected nucleosides **10–14** [11]. The isomeric purities of these products were found to be excellent as evident through their 500 MHz ^{1}H-NMR spectra (Figs. 1C–F and 2A–F) [11]. The deuterated ribonucleosides **11–14** were converted to the corresponding 2′-deoxynucleosides **15–18** [11]. The level of deuterium incorporation at the 2″ was > 97 atom % as evidenced by integration of ^{1}H-NMR spectra at 500 MHz (shown in Figs. 3A–F and 4A) of the residual proton resonance.

In order to investigate the effect of deuterium incorporation in the pentose moieties on the 1-D and 2-D ^{1}H-NMR spectra such as DQF-COSY, HOHAHA (TOCSY) and NOESY, eight sets of deuterated dimers UpA* **19**, CpG* **20**, ApU* **21**, GpC* **22**, d(TpA*) **23**, d(CpG*) **24**, d(ApT*) **25** and d(GpC*) **26** and their natural abundance counterparts and one trimer A*2′p5′A2′p5′A* **27** were synthesized [11] (* denotes the deuterated part in the molecule) using standard phosphotriester chemistry [13]. These partially deuterated dinucleotides and the trinucleotide were subsequently compared with the corresponding natural counterparts to evaluate the actual NMR simplifications achieved in the ^{1}H-NMR window part (Scheme 1) as a result of specific deuterium incorporation. We have already reported [11] the synthesis of all of these deuterated dimers **19–26** and trimer **27**, but we have only reported the NMR simplifications achieved in case of UpA* **19**, CpG* **20**, d(CpG*) **24** and the trimer A*2′p5′A2′p5′A* **27**.

We herein report the 1-D and 2-D NMR spectra of ApU* **21**, GpC* **22**, d(TpA*) **23**, d(ApT*) **25** and d(GpC*) **26** and their natural abundance counterparts (Figs. 4C–17). Comparison of these deuterated and non-deuterated spectra (Figs. 4C–17) show, in conjunction with the partially deuterated dimers published in Ref. 11, that the complexities of the natural-abundance dimers are very different from case to case depending upon the aglycone and the nucleotide sequence. Such a comparison is useful to establish the varied degree of resonance overlap and simplifications achieved in them. These comparative studies for partially deuterated dinucleotides may be of interest in the future studies as reference spectra in the interpretation of ^{1}H-NMR window in larger oligo-DNA and oligo-RNA. In addition, we have examined the deuterium isotope effect on the chemical shifts of H1′ and H4′ of the deuterated residue and 1′, 2′(2″), 3′, 4′, 5′/5″ in the non-deuterated residue in all partially deuterated dinucleotides and 2,5A core and compared with their natural abundance counterpart. Such a comparison shows (Table 1) that the chemical shifts of the H1′ and H4′ of the deuterated residue in **19–27** shift only by 0.01–0.02 ppm while the chemical shifts

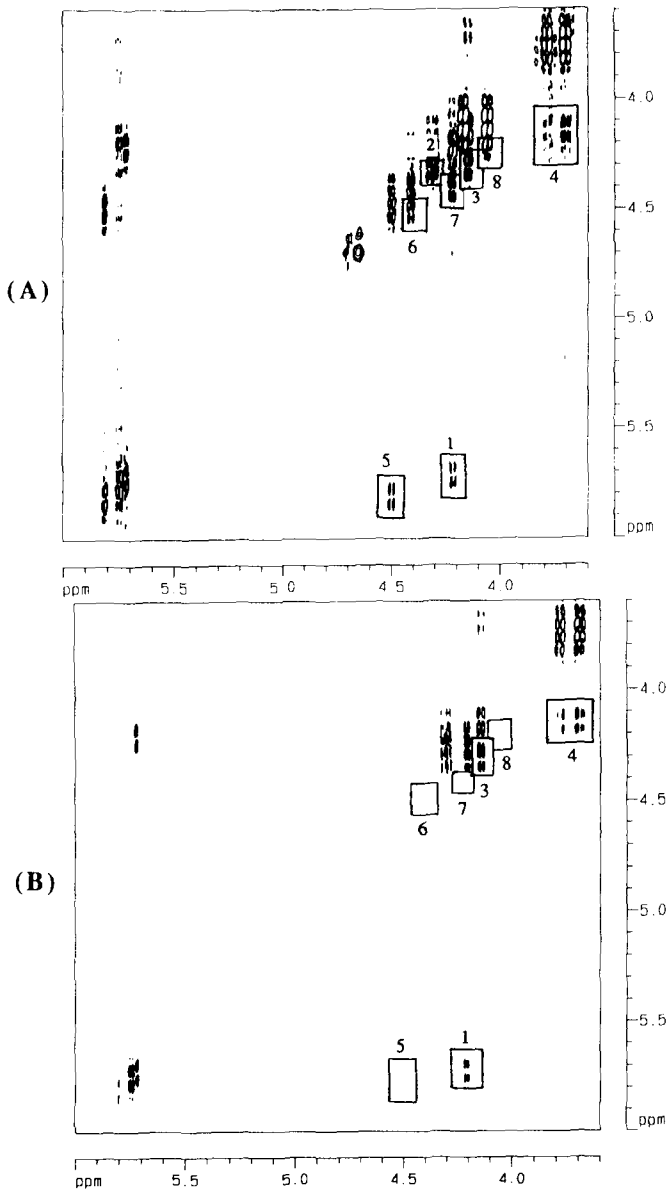

Fig. 14. DQF-COSY spectra of the natural and partially deuterated cytidylyl-(3′ → 5′)-guanosine (CpG) in D_2O at 298 K. Panel A: 2-D spectrum of the natural CpG. The cross peaks used for the determination of the vicinal $^3J_{HH}$ coupling constants are shown in the numbered boxes: (1) H1′C-H2′C, (2) H3′C-H4′C, (3) H2′C-H3′C, (4) H4′C-H5′C and H4′C-H5″C, (5) H1′G-H2′G, (6) H2′G-H3′G, (7) H3′G-H4′G, (8) H4′G-H5′G. Panel B: 2-D spectrum of CpG* where the $1'^{\#}$,2′,3′,$4'^{\#}$ and 5′/5″ of pG* have been exchanged with deuterium. The empty boxes show that all cross peaks involving the pG* residue have vanished.

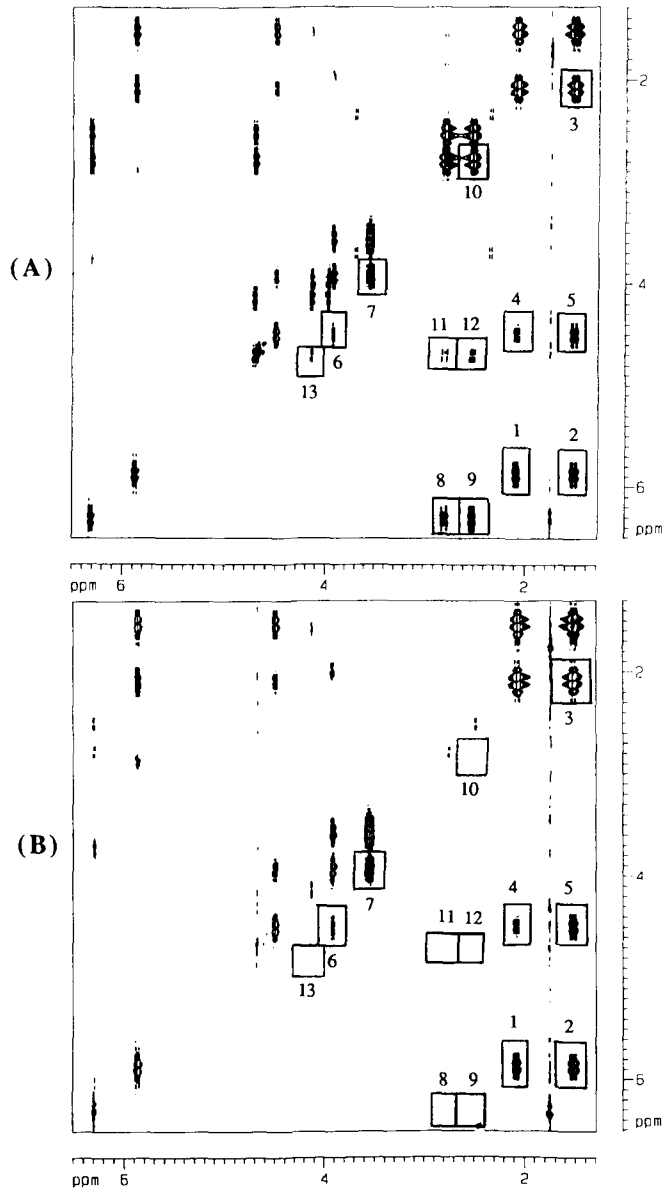

Fig. 15. DQF-COSY spectra of natural and partially deuterated thymidylyl-(3′ → 5′)-2′-deoxyadenosine (d(TpA)) in D_2O at 298 K. Panel A: 2-D spectrum of the natural d(TpA). The cross peaks used for the determination of the vicinal $^3J_{HH}$ coupling constants are shown in the numbered boxes: (1) H1′-H2″T, (2) H1′-H2′T, (3) H2′-H2″T, (4) H2″-H3′T, (5) H2′-H3′T, (6) H3′-H4′T, (7) H4′-H5′T, H4′-H5″T, (8) H1′-H2′A, (9) H1′-H2″A, (10) H2′-H2″A, (11) H2′-H3′A, (12) H2″-H3′A, (13) H3′-H4′A. Panel B: 2-D spectrum of d(TpA*) where the 1′#,2′,2″,3′,4′# and 5′/5″ of pA* have been exchanged with deuterium. The empty boxes show that all cross peaks involving the pA* residue have vanished.

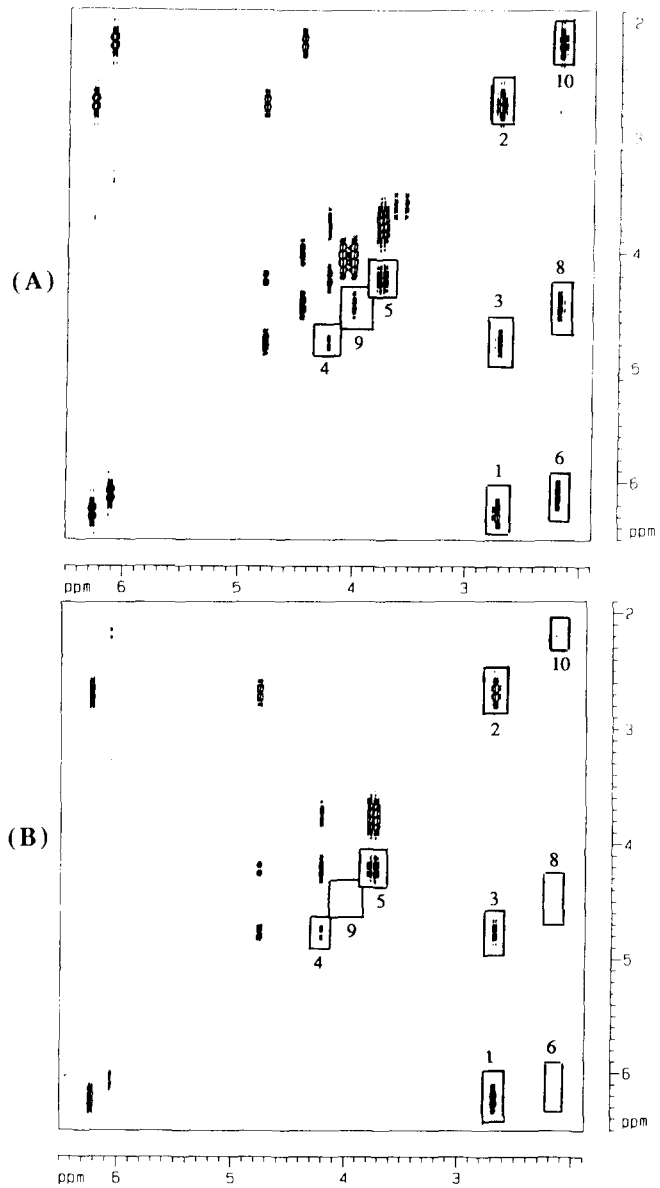

Fig. 16. DQF-COSY spectra of natural and partially deuterated 2′-deoxyadenylyl-(3′ → 5′)-thymidine (d(ApT)) in D_2O at 298 K. Panel A: 2-D spectrum of the natural d(ApT). The cross peaks used for the determination of the vicinal $^3J_{HH}$ coupling constants are shown in the numbered boxes: (1) H1′-H2′A, H1′-H2″A, (2) H2′-H2″A, (3) H2′-H3′A, H2″-H3′A, (4) H3′-H4′A, (5) H4′-H5′A, H4′-H5″A, (6) H1′-H2′T, H1′-H2″T, (7) H2′-H2″T, (8) H2′-H3′T, H2″-H3′T, (9) H3′-H4′T. Panel B: 2-D spectrum of d(ApT*) where the $1'^{\#}$,2′,2″,3′,$4'^{\#}$ and 5′/5″ of pT* have been exchanged with deuterium. The empty boxes show that all cross peaks involving the pT* residue have vanished.

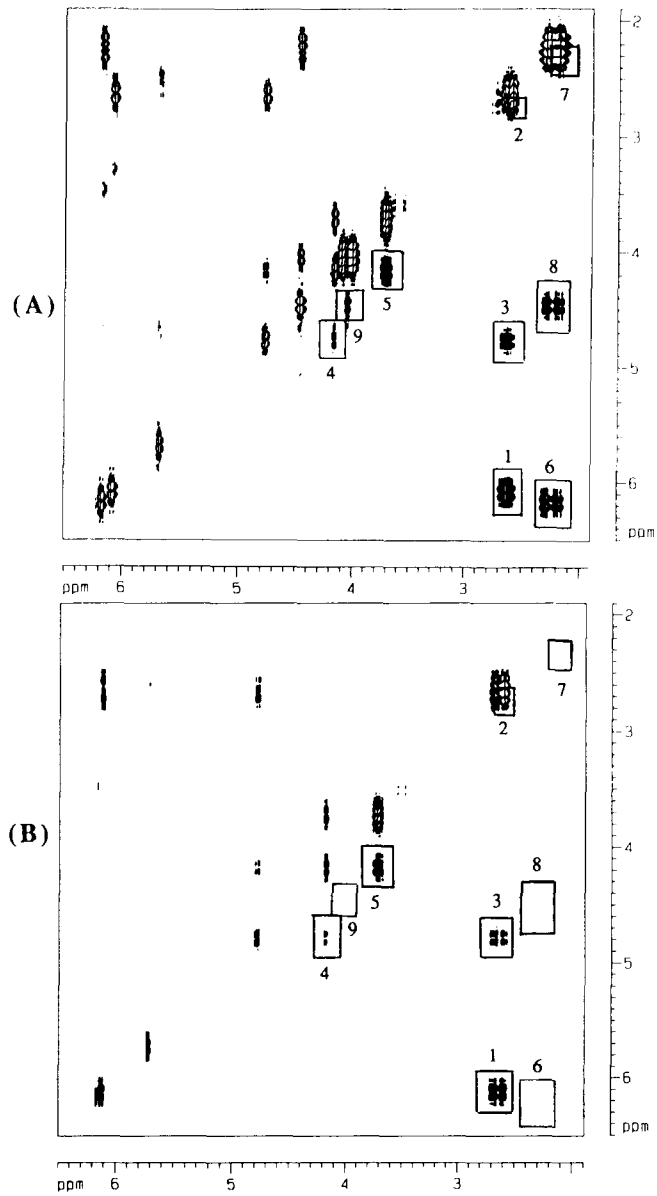

Fig. 17. DQF-COSY spectra of natural and partially deuterated 2′-deoxyguanylyl-(3′ → 5′)-2′-deoxycytidine (d(GpC)) in D_2O at 298 K. Panel A: 2-D spectrum of the natural d(GpC). The cross peaks used for the determination of the vicinal $^3J_{HH}$ coupling constants are shown in the numbered boxes: (1) H1′-H2′G, H2″-H3′G, (2) H2′-H2″G, (3) H2′-H3′G, H2″-H3′G, (4) H3′-H4′G, (5) H4′-H5′G, H4′-H5″G, (6) H1′-H2′C, H1′-H2″C, (7) H2′-H2″C, (8) H2′-7H3′C, H2″-H3′C, (9) H3′-H4′C. Panel B: 2-D spectrum of d(GpC*) where the $1'^{\#}$,2′,2″,3′,$4'^{\#}$ and 5′/5″ of pC* have been exchanged with deuterium. The empty boxes show that all cross peaks involving the pC* residue have vanished.

TABLE 1

^{1}H chemical shifts (δ scale, reference: δ(acetonitrile) = 2.00 ppm) of partially deuterated oligomers and their comparison (deuterium isotope effect) with the natural-abundance counterparts in D_2O at 298 K (except for the trimer which is recorded at 308 K) at 3–8 mM concentrations

Oligomer	Residue	H1′	H2′	H2″	H3′	H4′	H5′	H5″	H8/H6	H2/H5/Me[5]
UpA	U	5.84	4.28	–	4.51	4.20	3.80	3.75	7.65	5.78
	A	6.14	4.79	–	4.57	4.41	4.26	4.19	8.45	8.25
UpA* **19**	U	5.86	4.27	–	4.51	4.19	3.79	3.75	7.62	5.78
	A*	6.14	–	–	–	4.40	–	–	8.46	8.26
CpG	C	5.88	4.21	–	4.31	4.15	3.79	3.70	7.59	5.75
	G	5.97	4.50	–	4.41	4.37	4.17	4.06	7.92	–
CpG* **20**	C	5.88	4.21	–	4.31	4.15	3.79	3.69	7.59	5.74
	G*	5.97	–	–	–	4.37	–	–	7.91	–
ApU	A	6.02	4.38	–	4.63	4.42	3.94	3.83	8.29	8.15
	U	5.75	4.24	–	4.20	4.19	4.26	4.08	7.67	5.60
ApU* **21**	A	6.03	4.84	–	4.63	4.42	3.93	3.83	8.30	8.17
	U*	5.75	–	–	–	4.18	–	–	7.67	5.60
GpC	G	5.80	4.74	–	4.61	4.35	3.89	3.79	7.89	–
	C	5.84	4.22	–	4.19	4.16	4.29	4.07	7.75	5.71
GpC* **22**	G	5.81	4.74	–	4.61	4.35	3.90	3.79	7.91	–
	C*	5.84	–	–	–	4.17	–	–	7.75	5.71
D(TpA)	T	5.9	2.11	1.55	4.53	3.95	3.60	3.56	7.27	1.78
	dA	6.34	2.82	2.54	4.73	4.17	4.0	4.0	8.32	8.07

d(TpA*) **23**	T	5.90	2.11	1.55	4.53	3.95	3.61	3.57	7.27	1.78
	dA*	6.33	–	–	–	4.16	–	–	8.32	8.06
d(CpG)	dC	6.0	2.27	1.62	4.51	4.01	3.60	3.55	7.51	5.86
	dG	6.14	2.76	2.46	4.13	4.13	3.95	3.93	7.93	–
d(CpG*) **24**	dC	6.05	2.28	1.63	4.52	4.02	3.63	3.57	7.52	5.91
	dG*	6.18	–	–	–	4.13	–	–	7.98	–
d(ApT)	dA	6.30	2.73	2.73	4.82	4.26	3.81	3.75	8.18	8.06
	T	6.14	2.23	2.23	4.49	4.02	4.14	4.03	7.39	1.68
d(ApT*) **25**	dA	6.29	2.73	2.73	4.83	4.29	3.82	3.75	8.18	8.04
	T*	6.13	–	–	–	4.01	–	–	7.40	1.68
d(GpC)	dG	6.13	2.73	2.63	4.80	4.20	3.77	3.73	7.88	–
	dC	6.21	2.33	2.22	4.50	4.08	4.13	4.04	7.69	5.72
d(GpC*) **26**	dG	6.15	2.72	2.63	4.81	4.21	3.78	3.73	7.90	–
	dC*	6.20	–	–	–	4.07	–	–	7.71	5.75
A2′p5′A2′p5′A	A-2′p	6.11	5.05	–	4.58	4.23	3.84	3.72	8.13	7.85
	pAp	5.97	4.85	–	4.58	4.18	4.06	3.89	8.02	7.98
	5′p-A	5.88	4.45	–	4.33	4.25	4.16	4.11	8.03	8.24
A*2′p5′A2′p5′A*	A*-2′p	6.10	–	–	–	4.22	–	–	8.13	7.85
27	pAp	5.97	4.84	–	4.57	4.17	4.06	3.90	8.02	7.97
	5′p-A*	5.87	–	–	–	4.24	–	–	8.02	8.24

* Denotes the deuterated sugar moiety. See text and Ref. 11.

of the non-deuterated moiety move by $\leqq 0.01$ ppm due to deuterium isotope effect. Such a comparison shows that the deuterium isotope effect on proton chemical shifts is indeed very small. This means that it would be possible to overlay the spectrum of various 'NMR-window' containing analogues of deuterium-labeled oligo-DNA or RNA (as shown in Scheme 1) and compare the cross-peaks in multidimensional correlation or NOESY spectroscopy for the conformational studies without any problem due to the distortion of the chemical shifts from the deuterium isotope effect provided the concentration and the temperature are identical.

Simplified description of the method

The ^{1}H-NMR experiments were performed [11] on a Bruker AMX-500 MHz spectrometer. The DQF-COSY and Hartmann-Hahn spectra were recorded in pure-phase absorption mode with the time proportional incrementation method (TPPI) and with low power preirradiation of the residual HDO peak during the relaxation delay. The DQF-COSY [15] spectra were acquired with 4096 complex data points in t_2 and 256 points in t_1. The data were zero filled to give a 4096×1024 point matrix and a sine-square bell window was applied in both directions before Fourier transformation. The Hartmann-Hahn [16] spectra were acquired with 2048 complex data points in t_2 and 256 points in t_1. The data were zero filled to give a 2048×1024 point matrix and a sine-square bell window was applied in both directions before Fourier transformation.

Acknowledgements

The authors thank the Swedish Board for Technical Development (NUTEK) and Swedish Natural Science Research Council for generous financial support. We also thank Wallenbergstiftelsen, University of Uppsala, Forskningsrådsnämnden (FRN) for financial supports for purchasing the 500 MHz NMR spectrometer.

References

1 Saenger, W. (1983) Principles of Nucleic Acid Structure, Springer-Verlag, New York.
2a Jardetzky, O. and Roberts, G.C.K. (1981) NMR in Molecular Biology, Academic Press, New York, Ch. 13.
2b Wemmer, D.E. and Reid, B.R. (1985) Ann. Rev. Phys. Chem. 36, 105.
2c Wüthrich, K. (1986) NMR of Proteins and Nucleic Acids, Wiley, New York.
2d Reid, B.R. (1987) Q. Rev. Biophys. 20, 1.
2e Van de Ven, F.J.M. and Hilbers, C.W. (1988) Eur. J. Biochem. 178, 1.
2f Hosur, R.V., Govil, G. and Miles, H.T. (1988) Magn. Reson. Chem. 26, 927.
3a Weiner, P.K. and Kollman, P.A. (1981) J. Comp. Chem. 2, 287.
3b Weiner, S.J., Kollman, P.A., Nguyen, D.T. and Case, D.A. (1986) J. Comp. Chem. 7, 230.
4a Ernst, R.R., Bodenhausen, G. and Wokaun, A. (1987) Principles of Nuclear Magnetic Resonance in One and Two Domensions, Clarendon Press, Oxford.
4b Oppenheimer, N.J. and James, T.L. (Eds.) (1989) Methods Enzymol. 176, Ch. 1 and 2.
5a Neuhaus, D. and Williamson, M.P. (1989) The Nuclear Overhauser Effect in Structural and Conformational Analysis, VHC Publishers, New York.

5b James, T.L. (1991) Current Opinion in Structural Biology, 1, 1042.
5c Torda, A.E., Scheek, R.M. and van Gunsteren, W.F. (1990) J. Mol. Biol. 214, 223.
5d Kaluarachchi, K., Meadows, R.P., Gorenstein, D.G. (1991) Biochemistry 30, 8785.
5e Pearlman, D.A. and Kollman, P.A. (1991) J. Mol. Biol. 220, 457.
6a Vuister, G.W. and Boelens, R. (1987) J. Magn. Reson. 73, 328.
6b Mooren, M.M.W., Hilbers, C.W., Van Der Marel, G.A., Van Boom, J.H. and Wijmenga, S.S. (1991) J. Magn. Reson. 94, 101.
6c Majumdar, A. and Hosur, R.V. (1991) J. Biomol. NMR 1, 205.
6d Sörensen, O.W. (1990) J. Magn. Reson. 90, 433.
7a Schmidt, R.R., Heermann, D. and Jung, K.-H. (1974) Liebigs Ann. Chem. 1856.
7b Fraser-Reid, B. and Radatus, B. (1971) J. Am. Chem. Soc. 93, 6342.
7c Radatus, B., Yunker, M. and Fraser-Reid, B. (1971) J. Am. Chem. Soc. 93, 3086.
7d David, S. and Eustache, J. (1971) Carbohyd. Res. 16, 469.
7e David, S. and Eustache, J. (1971) Carbohyd. Res. 20, 319.
7f Wong, M.Y.H. and Gray, G.R. (1978) J. Am. Chem. Soc. 100, 3548.
7g Pathak, T., Bazin, H. and Chattopadhyaya, J. (1986) Tetrahedron 42, 5427.
7h Roy, S., Hiyama, Y., Torchia, D.A. and Cohen, J.S. (1986) J. Am. Chem. Soc. 108, 1675.
7i Wu, J.-C., Bazin, H. and Chattopadhyaya, J. (1987) Tetrahedron 43, 2355.
7j Hodge, R.P., Brush, C.K., Harris, C.M. and Harris, T.M. (1991) J. Org. Chem. 56, 1553.
7k Kline, P.C. and Serianni, A.S. (1988) Magn. Reson. Chem. 26, 120.
7l Kline, P.C. and Serianni, A.S. (1990) Magn. Reson. Chem. 28, 324.
7m Pathak, T. and Chattopadhyaya, J. (1987) Tetrahedron 43, 4227.
8a Schmidt, R.R., Scholz, U. and Schwille, D. (1968) Chem. Ber. 101, 590.
8b Dupre, M. and Gaudemer, A. (1978) Tetrahedron Lett. 2783.
8c Kintanar, A., Alam, T.M., Huang, W.-C., Schindele, D.C., Wemmer, D.E. and Drobny, G. (1988) J. Am. Chem. Soc. 110, 6367.
8d Berger, A., Shaw, A. and Cadet, J. (1987) Nucleosides Nucleotides 6, 395.
8e Ajmera, S., Massof, S. and Kozarich, J.W. (1986) J. Labelled Compd. 23, 963.
8f Sinhababu, A.K., Bartel, R.L., Pochopin, N. and Borchardt, R.T. (1985) J. Am. Chem. Soc. 107, 7628.
8g Robins, M.J., Samano, V. and Johnson, M.D. (1990) J. Org. Chem. 55, 410.
8h Kondo, N.S. and Danyluk, S.S. (1972) J. Am. Chem. Soc. 94, 5121.
8i Kondo, N.S., Leung, A. and Danyluk, S.S. (1973) J. Labelled Compd. 9, 497.
8j Kondo, N.S., Ezra, F. and Danyluk, S.S. (1975) FEBS Lett. 53, 213.
8k Kondo, N.S. and Danyluk, S.S. (1976) Biochemistry 15, 756.
8l Lee, C.-H., Ezra, F., Kondo, N.S., Sarma, R.H. and Danyluk, S.S. (1976) Biochemistry 15, 3627.
8m Ezra, F.S., Lee, C.-H., Kondo, N.S., Danyluk, S.S. and Sarma, R.H. (1977) Biochemistry 16, 1977.
9a Brush, C.K., Stone, M.P. and Harris, T.M. (1988) Biochemistry 27, 115.
9b Brush, C.K., Stone, M.P. and Harris, T.M. (1988) J. Am. Chem. Soc. 110, 4405.
10a Hiyama, Y., Roy, S., Cohen, J.S. and Torchia, D.A. (1989) J. Am. Chem. Soc. 111, 8609.
10b Alam, T M. and Drobny, G. (1990) Biochemistry 29, 3421.
10c Alam, T.M., Orban, J. and Drobny, G. (1990) Biochemistry 29, 9610.
10d Huang, W.-C., Orban, J., Kintanar, A., Reid, B.R. and Drobny, G.P. (1990) J. Am. Chem. Soc. 112, 9059.
10e Alam, T.M., Orban, J. and Drobny, G.P. (1991) Biochemistry 30, 9229.
11 Földesi, A., Nilson, F.P.R., Glemarec, C., Gioeli, C. and Chattopadhyaya, J. (1992) Tetrahedron, in press.
12a Koch, H.J. and Stuart, R.S. (1977) Carbohydr. Res. 59, C1.
12b Balza, F., Cyr, N., Hamer, G.K., Perlin, A.S., Koch, H.J. and Stuart, R.S. (1977) Carbohydr. Res. 59, C7.
12c Koch, H.J. and Stuart, R.S. (1978) Carbohydr. Res. 64, 127.
12d Koch, H.J. and Stuart, R.S. (1978) Carbohydr. Res. 59, 341.
12e Balza, F. and Perlin, A.S. (1982) Carbohydr. Res. 107, 270.
12f Angyal, S.J. and Odier, L. (1983) Carbohydr. Res. 123, 13.

12g Wu, G.D., Serianni, A.S. and Barker, R. (1983) J. Org. Chem. 48, 1750.
12h Angyal, S.J., Stevens, J.D. and Odier, L. (1986) Carbohydr. Res. 157, 83.
13a Reese, C.B. (1978) Tetrahedron 34, 3143.
13b Sandström, A., Kwiatkowski, M. and Chattopadhyaya, J. (1985) Acta Chem. Scand. B39, 273.
13c Chattopadhyaya, J. and Reese, C.B. (1979) Tetrahedron Lett. 5059.
13d Kwiatkowski, M., Heikkilä, J., Björkman, S. and Chattopadhyaya, J. (1983) Chemica Scripta 22, 30
13e Zhou, X.X., Sandström, A. and Chattopadhyaya, J. (1986) Chemica Scripta 26, 241.
13f Jones, S.S., Rayner, B., Reese, C.B., Ubasawa, A. and Ubasawa, M. (1980) Tetrahedron 36, 3075
13g Reese, C.B., Titmus, R.C. and Yau, L. (1978) Tetrahedron Lett. 2727.
14a Bax, A. and Freeman, R. (1981) J. Magn. Reson. 44, 542.
14b Aue, W.P., Batholdi, E. and Ernst, R.R. (1976) J. Chem. Phys. 64, 2229.
15 Piantini, O.W., Sorensen, O.W. and Ernst, R.R. (1982) J. Am. Chem. Soc. 104, 6800.
16 Bax, A., Griffey, R.H. and Hawkins, B.L. (1981) J. Magn. Reson. 42, 501.